Decanedioic Acid ($C_{10}H_{18}O_4$)/Dodecanedioic Acid ($C_{12}H_{22}O_4$) System: Polymorphism of the Components and Experimental Phase Diagram

by **Lourdes Ventolà***, **Laura Bayés**, **Raül Benages**, **Francisco Javier Novegil-Anleo**, **Miquel Ángel Cuevas-Diarte**, and **Teresa Calvet**

Departament de Cristal·lografia, Mineralogia i Dipòsits Minerals, Facultat de Geologia, Universitat de Barcelona, Martí i Franquès s/n, E-08028, Barcelona
(phone: +34 934021350; fax: +34 934021340; e-mail: lourdes_ventola@yahoo.com)

and

Denise Mondieig

Centre de Physique Moléculaire Optique et Hertzienne, UMR 5798 au CNRS Université Bordeaux I, Cours de la Libération 351, F-33405, Talence Cedex

The experimental temperature/composition phase diagram of the binary system decanedioic acid ($C_{10}H_{18}O_4$)/dodecanedioic acid ($C_{12}H_{22}O_4$) was established by combining X-ray powder diffraction (XRD), differential-scanning calorimetry (DSC), infrared spectroscopy (IR), scanning electron microscopy (SEM), and thermo-optical microscopy (TOM). Both compounds crystallize in the same ordered form, C ($P2_1/c$), which is the phase that melts in both cases. The C form melts in $C_{12}H_{22}O_4$ earlier than in $C_{10}H_{18}O_4$, in contrast to other unbranched-chain compounds (alkanes, alkanols, and alkanoic acids) in which the melting temperatures increase as the C-atom number rises. Contrary to what might be expected, total solid-state miscibility is not observed. The $C_{10}H_{18}O_4/C_{12}H_{22}O_4$ binary system shows a complex phase diagram. At low temperatures, a new monoclinic form, C_i ($P2_1/c$), stabilizes as a result of the disorder of composition in the mixed samples; two [$C + C_i$] domains appear. Upon heating, four solid–solid and seven solid–liquid domains appear related by eutectic and peritectic invariants. All the crystallographic forms observed are isostructural.

1. Introduction. – We present here part of a general study on organic-solid-state miscibility, undertaken a few years ago within our research group and the REALM[1]) (= *Réseau Européen sur les Alliages Moléculaires*) collaborating laboratories.

We are interested in the preparation of molecular mixed crystals, the study of their crystallographic and thermodynamic properties and stability, the determination of their solid-state miscibility, and their practical applications [1–6]. Therefore, our research is invariably focused on the study of different families of molecular substances, such as naphthalene derivatives, benzene derivatives, unbranched alkanes, alkanols, and alkanoic acids, and in this case unbranched alkanedioic acids.

Alkanedioic acids ($HOOC(CH_2)_nCOOH$) are unbranched-chain molecules with COOH groups at both ends. A very long one-dimensional chain can be formed through H-bond formation at both ends. Alkanedioic acids form a layered structure in the solid

[1]) The REALM assembles four European Universities: Universitat de Barcelona, Universitat Politècnica de Catalunya, Utrecht University, and Université Bordeaux I.

state, as do most polymorphic phases of long-chain compounds, such as unbranched alkanes, alkanols, and alkanoic acids [7–12]. Owing to the presence of COOH groups at both ends of the chain, the density of H-bonds is significantly greater than in alkanoic acids. That could explain why their melting points are higher than those of analogous alkanoic acids: dodecanoic acid melts at 317.3 K, while dodecanedioic acid melts at 401 K [7].

Alkanedioic acids show a marked difference in the melting points of the shorter odd- and even-number diacids (*i.e.*, consisting of an odd or even number of C-atoms, resp.), which converge as the chain length reaches 20 C-atoms. The odd-number diacids have a rather monotonous increase in melting points with increasing chain length, while the even-number diacids have sharply decreasing melting points as the chain lengthens [7].

Two polymorphic forms α ($P2_1/c$) in the even- and odd-number series, and β ($C2/c$) only in the odd-number series have been described in the literature [9][10][13][14]. The gross structural features are similar in the even- and (both forms of) odd-number series of alkanedioic acids [13]: *i*) COOH Groups form H-bonded dimers at both ends of the molecules, leading to infinite chains. *ii*) CH_2 Chains stack into columns through hydrophobic interactions. However, there are certain differences within these similar packing patterns that are important in the context of melting-point alternation: *i*) Molecules are offset along their length within the columnar stacks in the even-number series, whereas such an offset is absent in both forms of the odd-number series. *ii*) Molecules in both modifications of the odd-number series exhibit twisted molecular conformations with severe torsions as opposed to the nontwisted all-*trans* conformation in the even-number series.

The IR spectra showed that the solid states of unbranched alkanedioic acids bore a marked structural similarity to those of alkanoic acids. This is why in some reports [15–19], the same nomenclature is used to describe the different forms[2]): *B*, *C*, *E* ($P2_1/c$), and *A* ($P\bar{1}$). The hydrocarbon chains take the all-*trans* conformation in the *A*, *C*, and *E* forms, while the *B* form has a *gauche* conformation in the vicinity of the COOH group [15][20]. The A_{super} form has an unusual conformation, in which the COOH group rotates about the C(1)–C(2) bond. This structure is explained by the O,O-distance of the adjacent molecule [20].

The present paper deals with the study of the $C_{10}H_{18}O_4$ and $C_{12}H_{22}O_4$ polymorphism and the experimental determination of the binary phase diagram between these two compounds. We followed a complementary approach, including X-ray powder diffraction (XRD), differential-scanning calorimetry (DSC), infrared spectroscopy (IR), scanning electron microscopy (SEM), and thermo-optical microscopy (TOM).

To the best of our knowledge, the phase diagram of the $C_{10}H_{18}O_4/C_{12}H_{22}O_4$ binary system has been reported only once in the literature. There, a complete range of miscibility at high temperature was observed, and only a solid–solid domain was recognized for compositions rich in $C_{12}H_{22}O_4$ at low temperatures [10].

2. Experimental. – *General.* The two alkanedioic acids $C_{10}H_{18}O_4$ and $C_{12}H_{22}O_4$ were purchased from *Fluka Chemical* as $\geq$99.5% pure and used without further purifications. Purity was corroborated by gas

[2]) As it is the case in the present paper.

chromatography (GC). Twenty-three mixed samples were obtained by 'melting–quenching': The components were weighed in the desired proportions, melted, and mixed to a homogeneous solution, and then quenched in liquid N_2.

Differential-Scanning Calorimetry (DSC). *Perkin-Elmer DSC-7* calorimeter; conditions: sample weight between 3.9 and 4.1 mg and scanning rate 2 K min^{-1}. Six independent measurements were performed for each sample. The instrument was calibrated by reference to the enthalpy and m.p. of indium and decane standards. The random part of the uncertainties was estimated with *Student*'s method, with a 95% threshold of reliability. The characteristic temp. were determined from the DSC curves by the shape-factor method [21]. Enthalpy effects were evaluated by integration of the DSC signals.

X-Ray Powder Diffraction Measurements (XRD). *Panalytical* and *Siemens D-500* diffractometers. Spectra were recorded on the *Panalytical* diffractometer at r.t. to improve resolution and minimize orientation effects. The *Panalytical* diffractometer was operated in transmission mode with CuK_α radiation by means of a double Mo crystal as the primary monochromator, and the sample was mounted in a sealed capillary of 0.5 mm diameter which rotated perpendicularly to the X-ray radiation beam. Variable-temp. measurements were recorded with the *Siemens D-500* diffractometer by means of *Bragg–Brentano* geometry, CuK_α radiation, and a secondary monochromator. The data were collected with an Anton PAAR TTK system, with a heating rate of 0.02 K s^{-1} and 5 min of stabilization time. Samples were heated from 298 K to the melting point. The patterns were scanned with a step size of 0.025° and step time of 5 s; the 2θ range was 1.6–60°. In both cases, the cell parameters were refined with the *Pawley* profile-fitting procedure option [22] of the Materials Studio software [23].

IR Spectroscopy. Bomem-DA3-FTIR spectrometer. The samples were finely powdered and measured at r.t. by means of a diffuse reflection accessory (DRIFT) within 450–4000 cm^{-1}. The resolution was 4 cm^{-1}, and all spectra were run in vacuum mode. The detector was an MCT (wide range), the beam splitter was KBr, and the source was a glow bar. Each spectrum was obtained by averaging 100 scans.

Scanning Electron Microscopy (SEM). *Hitachi S-4100* (field emission). The polycrystalline samples were mounted on a support platform of 12 mm diameter with a conductor adhesive (*Agar Scientific*), and fixed with a thin carbon layer of *ca.* 20 nm. SEM analyses were done at r.t.

Thermo-Optical Microscopy (TOM). *Linkam THMSG600* stage, mounted on a *Carl-Zeiss* microscope. The sample was placed on a 7 mm quartz cover slip and encased within a pure Ag lid so that it was heated from all sides, ensuring a uniform temp.

3. Results and Discussion. – *Pure Component Properties.* $C_{10}H_{18}O_4$ and $C_{12}H_{22}O_4$ do not exhibit polymorphism in the range of temperature and pressure studied. Both of them crystallize in the same monoclinic form *C* ($P2_1/c$, $Z=2$) [9][10][13][14]. This crystalline form is observed in all unbranched even-number alkanedioic acids with chain lengths ranging from C_4 to C_{16} [1][9][10][12–14][16][24][25]. The temperature and enthalpies of $C_{10}H_{18}O_4$ and $C_{12}H_{22}O_4$ measured are listed in *Table 1*, together with values from the literature.

The XRD results do not conclusively allow to identify the *C* form by analogy to the forms observed for the unbranched alkanoic acids. This is because the *E*, *B*, and *C* forms observed for the alkanoic acids are all monoclinic $P2_1/c$ [26–33]. IR Spectroscopy, SEM, and TOM are needed to understand the $C_{10}H_{18}O_4/C_{12}H_{22}O_4$ system. Crystal cell parameters of these two compounds are reported in *Table 2*.

The IR spectra, by analogy to the unbranched alkanoic acids [34–36] and other unbranched alkanedioic acids [16], indicate that both pure compounds adopt the *C* form at room temperature: *i*) The $r(CH_2)$ band splits into a doublet at 730 and 720 cm^{-1} due to the $O_\perp$ subcell. *ii*) The δ(OCO) band appears at 688 cm^{-1}, and the peak of the σ(O–H) band is at *ca.* 945 cm^{-1}.

Table 1. *Temperatures T_{fus} and Enthalpy Transitions (ΔH_{fus}) for $C_{10}H_{18}O_4$ and $C_{12}H_{22}O_4$*

	T_{fus} [K]	ΔH_{fus} [kJ mol^{-1}]	Ref.
$C_{10}H_{18}O_4$		40.5(5)	[10]
		43.9(4)	[1]
	404.0	40.8	[25]
	407.6		[7]
	406.6		[26]
	405.7(4)	46.9(1)	this work
$C_{12}H_{22}O_4$	402.1	53.4(6)	[10]
	402.5	50.5	[25]
		53.8(5)	[1]
	401.1		[7]
	401.6(3)	52.5(1)	this work

Table 2. *Cell Parameters for $C_{10}H_{18}O_4$ and $C_{12}H_{22}O_4$*. All the forms are monoclinic $P2_1/c$, $Z=2$.

	a [Å]	*b* [Å]	*c* [Å]	β [°]	Ref.
$C_{10}H_{18}O_4$	10.9936(10)	4.9858(5)	10.1403(10)	90.834(2)	[13]
	11.083(3)	4.987(1)	10.189(3)	90.01	[10]
	10.96	5.0	10.07	91.20	[9]
	10.9863(4)	4.9883(1)	10.1396(2)	90.788(1)	this work
$C_{12}H_{22}O_4$	13.16(2)	4.93(1)	10.20(1)	97.14	[9]
	13.137	4.933	10.174	97.19	[10]
	13.105(7)	4.921(2)	10.183(3)	97.40(3)	[14]
	13.1068(4)	4.9338(1)	10.1849(2)	97.297(1)	this work

The SEM results show regular prismatic plates for the two alkanedioic acids (*Fig. 1*), with an acute angle of 54°, characteristic of the *C* form, as observed for unbranched alkanoic acids [37][38].

Binary Phase Diagram. To understand the experimental phase diagram (*Fig. 2*), DSC, XRD, and TOM techniques were used. Twenty-three binary mixed samples (1-*x*)

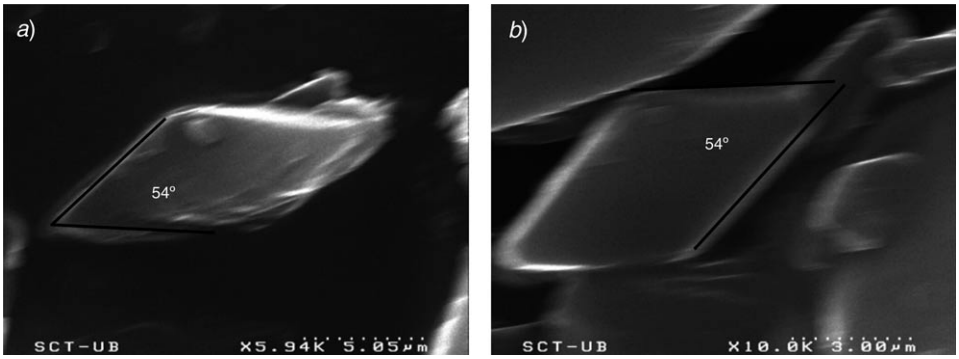

Fig. 1. *SEM Images of* a) *$C_{10}H_{18}O_4$ and* b) *$C_{12}H_{22}O_4$ at 298 K*

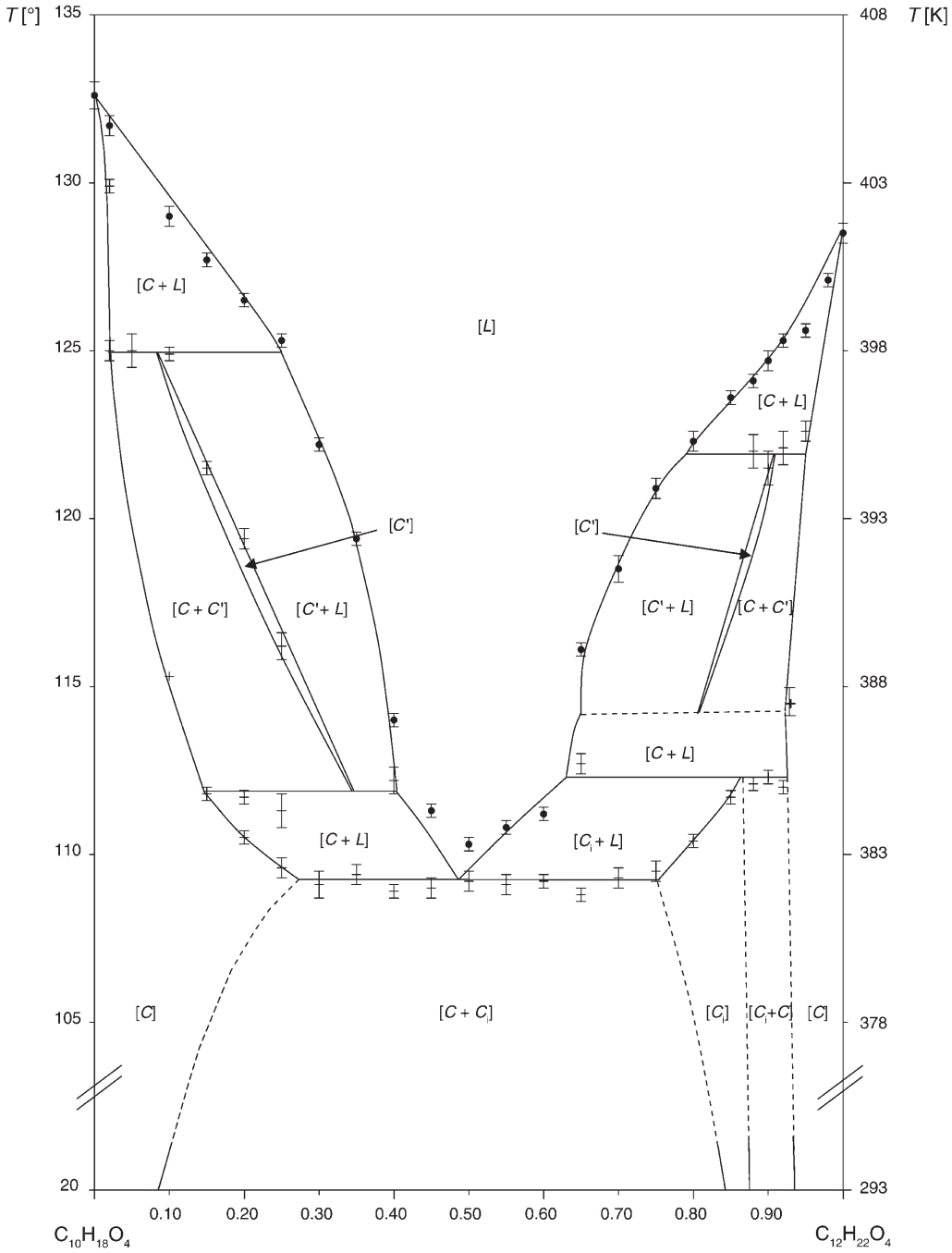

Fig. 2. *Experimental phase diagram of the $C_{10}H_{18}O_4/C_{12}H_{22}O_4$ binary system.* Abscissa, mol fraction *x* of $C_{12}H_{22}O_4$.

$C_{10}H_{18}O_4 + (x)\ C_{12}H_{22}O_4$ were analyzed under isothermal and isoplethic conditions. Thermo-energetic data deduced from thermal analyses are given in *Table 3*.

The experimental phase diagram is characterized at room temperature by two solid–solid fields. One of these fields is larger in intermediate compositions, and the other is narrower in compositions rich in $C_{12}H_{22}O_4$. The $[C]$, $[C + C_i]$, $[C_i]$, $[C_i + C]$ and $[C]$ sequence is observed when increasing the percentage of $C_{12}H_{22}O_4$. The C phase is the stable form of two pure compounds, and the C_i phase appears as a consequence of compositional disorder. The C and C_i forms belong to the same space group ($P2_1/c$), so it is difficult to differentiate between them. By XRD, when the C and C_i forms coexist, the FWHM (= full width at half maximum) of the $h00$ *Bragg* reflections increases (*Fig. 3*). No differences between C and C_i are observed by IR spectroscopy. By SEM and optical microscopy, all the prismatic plates show an acute angle of 54°.

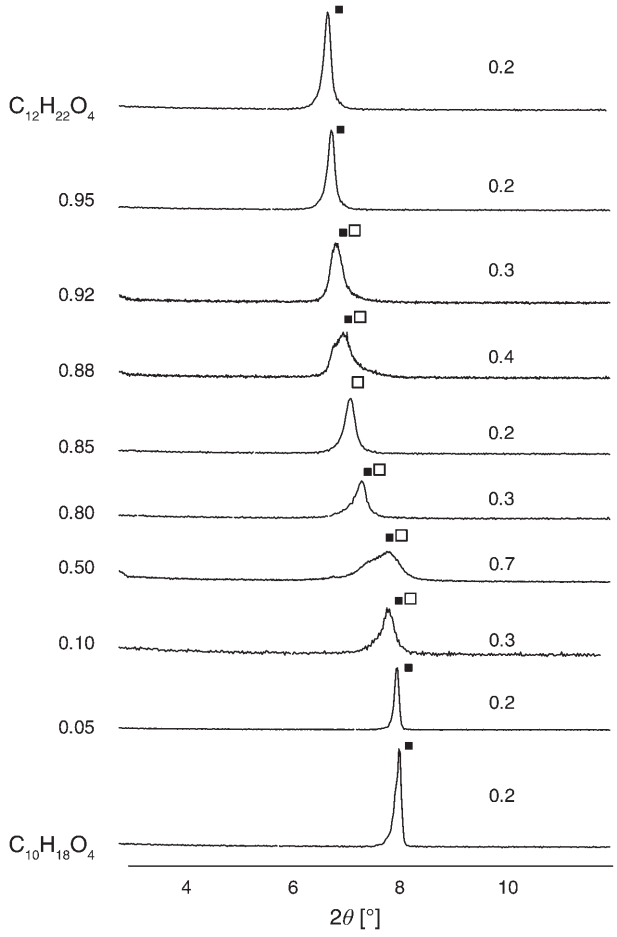

Fig. 3. *Full width at half maximum* (FWHM) *of the* h*00 reflexions as a function of composition.* ■, *C* form; □, C_i form. Left-hand scale, mol fraction x of $C_{12}H_{22}O_4$; right-hand scale, FWHM.

Table 3. *Temperatures T* [K] *and Enthalpy Transitions* ΔH [kJ mol^{-1}] *for the Mixed Compositions.* T_E and T_P are eutectic and peritectic invariants, resp.

	Mol-% $C_{12}H_{22}O_4$	T_{E1}	T_{E2}	T_{P1}	T_{P2}	T_{P3}	$T_{C\rightarrow L}$	$T_{Cl\rightarrow L}$	$T_{C\rightarrow C'}$	$T_{C'\rightarrow L}$	T_{sol}	T_{liq}	T_{fus}	ΔH_{fus}	ΔH_{tot}
$C_{10}H_{18}O_4$													405.7 ± 0.4	46.9 ± 1.2	
	2				398.1 ± 0.3						403.0 ± 0.2	404.8 ± 0.3			50.6 ± 1.0
	5				398.1 ± 0.5										53.1 ± 1.5
	10				398.0 ± 0.2				388.4 ± 0.2			402.1 ± 0.2			45.9 ± 1.3
	15		384.9 ± 0.2							394.6 ± 0.2		400.8 ± 0.2			45.2 ± 1.4
	20		384.8 ± 0.2				383.6 ± 0.2			392.5 ± 0.3		399.6 ± 0.2			44.4 ± 1.0
	25		384.4 ± 0.5				382.7 ± 0.3			389.3 ± 0.4		398.4 ± 0.2			44.3 ± 1.1
	30	382.2 ± 0.4										395.3 ± 0.2			43.2 ± 1.0
	35	382.5 ± 0.3										392.5 ± 0.2			42.7 ± 1.5
	40	382.0 ± 0.2	385.3 ± 0.4									387.1 ± 0.2			42.4 ± 1.2
	45	382.1 ± 0.3										384.4 ± 0.2			42.3 ± 1.4
	50	382.3 ± 0.3										383.4 ± 0.2			41.7 ± 1.0
	55	382.2 ± 0.3										383.9 ± 0.2			42.5 ± 1.2
	60	382.3 ± 0.2										384.3 ± 0.2			42.5 ± 1.0
	65	381.9 ± 0.2		385.8 ± 0.3								389.2 ± 0.2			41.7 ± 1.1
	70	382.4 ± 0.3										391.6 ± 0.4			42.8 ± 1.4
	75	382.6 ± 0.3										394.0 ± 0.3			43.9 ± 1.5
	80							383.5 ± 0.2				395.4 ± 0.3			43.9 ± 1.2
	85							384.8 ± 0.2				396.7 ± 0.2			44.7 ± 1.3
	88			385.2 ± 0.2		395.1 ± 0.5						397.2 ± 0.2			44.7 ± 1.2
	90			385.4 ± 0.2		394.6 ± 0.5						397.8 ± 0.3			45.5 ± 1.3
	92			385.1 ± 0.2		395.2 ± 0.5						398.4 ± 0.2			46.0 ± 1.5
	95								387.3 ± 0.5		395.7 ± 0.3	398.7 ± 0.2			47.6 ± 1.0
	98										398.5 ± 0.2	400.2 ± 0.2			50.6 ± 1.5
$C_{12}H_{22}O_4$	100												401.6 ± 0.3	52.5 ± 1.2	

Upon heating, a eutectic invariant is observed, covering a large part of the composition range (from *ca.* 30 to 80 mol-% of $C_{12}H_{22}O_4$) and located around T_{E1} 382.2 K (*Fig. 4,a*). Also upon heating, for compositions rich in $C_{10}H_{18}O_4$, an eutectic invariant (from *ca.* 15 to 40 mol-% of $C_{12}H_{22}O_4$) located at T_{E2} 384.7 K and a peritectic invariant (from *ca.* 2 to 25 mol-% of $C_{12}H_{22}O_4$) located at T_{P2} 398.0 K are observed (*Fig. 4,b*). As a result of the overlapping of different phenomena in the DSC signal, XRD isoplethic analysis for different compositions was required to establish the stability limits of the different phase domains as a function of temperature. As an example, *Fig. 5* shows the XRD measurements for a binary mixture containing 10 mol-% of $C_{12}H_{22}O_4$ at different temperatures; the results establish the following sequence: $[C+C_i]\rightarrow[C]\rightarrow[C+C']\rightarrow[C']\rightarrow[C'+L]\rightarrow[L]$. When two solid phases coexist, an increase in the FWHM for the *h*00 *Bragg* reflections and a shoulder for the 202 reflection are observed. When the liquid appears, an increase of the background spectrum and a displacement of the *Bragg* peaks as a consequence of the modification of the surface of diffraction are detected. Upon heating of compositions rich in $C_{12}H_{22}O_4$, a very similar phase-equilibria behavior as for compositions rich in $C_{10}H_{18}O_4$ is observed. Two peritectic invariants located at T_{P1} 385.2 K (from *ca.* 65 to 92 mol-% of $C_{12}H_{22}O_4$) and T_{P3} 395.0 K (from *ca.* 80 to 92 mol-% of $C_{12}H_{22}O_4$) are recognized (*Fig. 4,c*). As in the rest of the diagram, the overlapping phenomena in the DSC signals required the use of XRD measurements at different temperatures to establish the stability limits of the different phase domains. Measurements for a binary mixture containing 90 mol-% of $C_{12}H_{22}O_4$ at different temperatures are given in *Fig. 6*; the results establish the following sequence: $[C+C_i]\rightarrow[C+C']\rightarrow[C']\rightarrow[C+L]\rightarrow[L]$.

For the thermodynamic coherence of the binary phase diagram, a new eutectic invariant (E_3) is required to link the $[C+L]$, $[C'+L]$, and $[C+C']$ domains for compositions rich in $C_{12}H_{22}O_4$. This is placed at *ca.* 387 K, from 65 to 95 mol-% of $C_{12}H_{22}O_4$. The existence of the $[C+L]$ domain was corroborated by TOM analysis where in the mixture containing 90 mol-% of $C_{12}H_{22}O_4$, a liquid phase appears between *ca.* 385 and 387 K.

All the compositions studied show an acute angle of 54° for all the prismatic plates by TOM measurements.

Conclusions. – Neither decanedioic acid ($C_{10}H_{18}O_4$) nor dodecanedioic acid ($C_{12}H_{22}O_4$) presents polymorphism. Both compounds crystallize in the same ordered form *C*, belonging to the space group $P2_1/c$, with $Z=2$.

The experimental phase diagram exhibits a very low solubility in the solid state: *i*) five monophasic domains, *i.e.*, two $[C]$, two $[C']$, and one $[C_i]$; *ii*) four solid–solid domains, *i.e.*, two $[C_i+C]$ and two $[C+C']$; *iii*) six solid–liquid domains, *i.e.*, three $[C+L]$, two $[C'+L]$, and one $[C_i+L]$; *iv*) three eutectic invariants located at T_{E1} *ca.* 382.2 K between *x ca.* 30 and 75 mol-% of $C_{12}H_{22}O_4$, at T_{E2} *ca.* 384.7 K between *x ca.* 15 and 40 mol-% of $C_{12}H_{22}O_4$, and at T_{E3} *ca.* 387 K between *x ca.* 65 and 95 mol-% of $C_{12}H_{22}O_4$; *v*) three peritectic invariants located at T_{P1} *ca.* 385.2 K between *x ca.* 65 and 92 mol-% of $C_{12}H_{22}O_4$, at T_{P2} *ca.* 398.0 K between *x ca.* 2 and 25 mol-% of $C_{12}H_{22}O_4$, and at T_{P3} *ca.* 395.0 K between *x ca.* 80 and 92 mol-% of $C_{12}H_{22}O_4$; *i*)–*v*) explain the binary phase diagram.

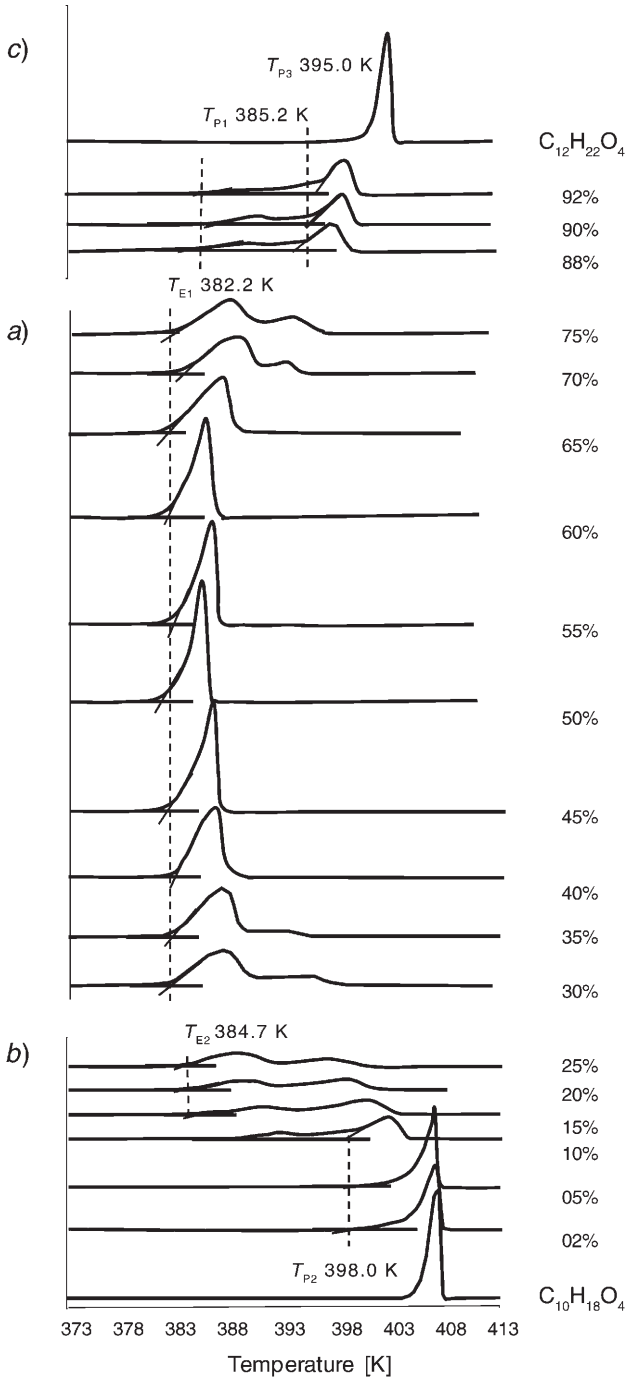

Fig. 4. *DSC Thermograms as a function of molar fraction in* $C_{12}H_{22}O_4$. Right-hand scale, mol-% $C_{12}H_{22}O_4$.

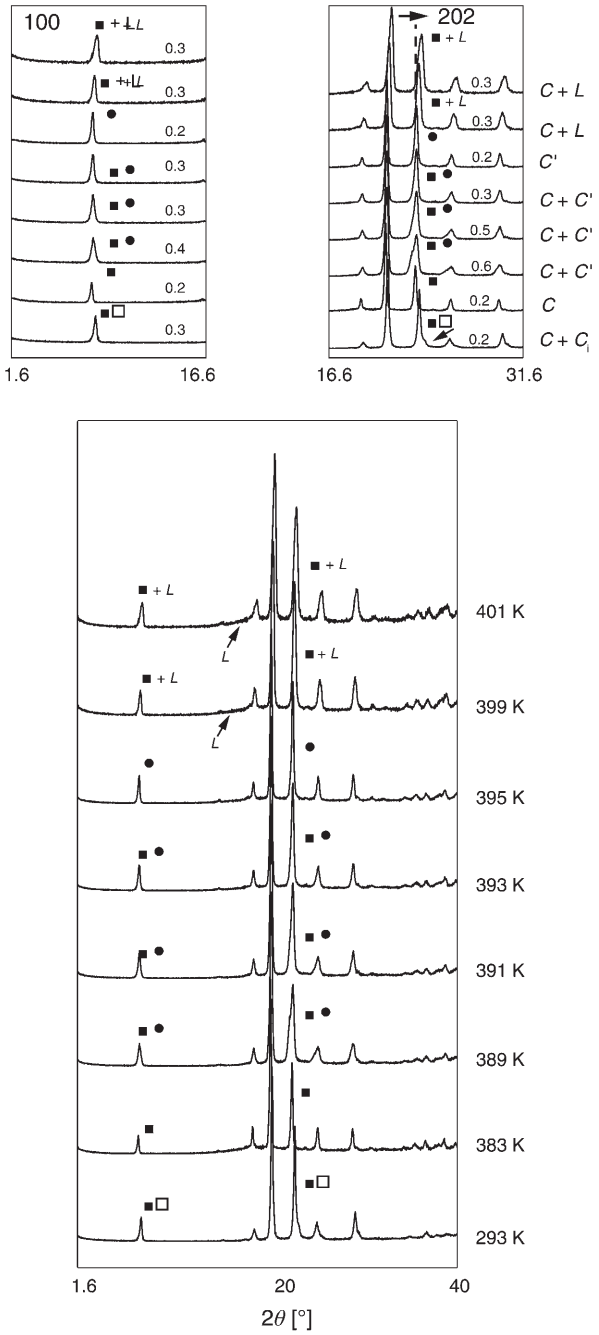

Fig. 5. *XRD Diagrams for the binary mixture* $C_{10}H_{18}O_4/C_{12}H_{22}O_4$ *9:1 as a function of temperature.* ■, *C* form; ●, *C′* form; □, C_i form.

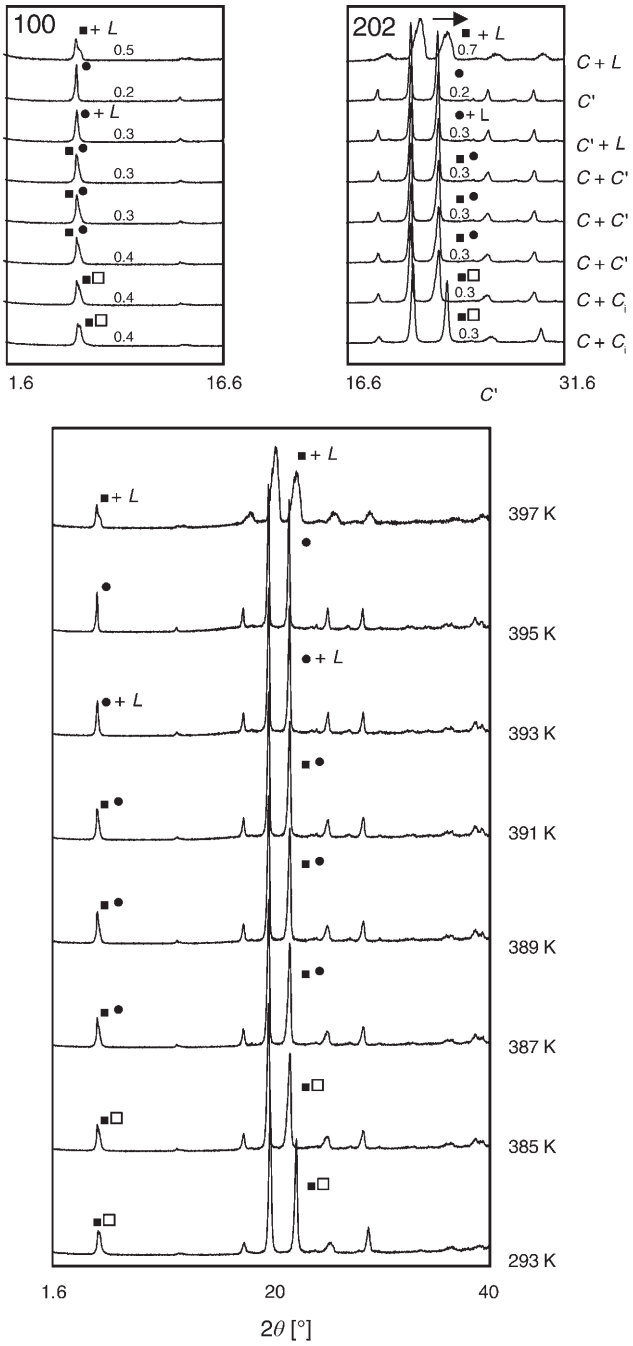

Fig. 6. *XRD Diagrams for the binary mixture* $C_{10}H_{18}O_4/C_{12}H_{22}O_4$ *1:9 as a function of temperature.* ■, *C* form; ●, *C′* form; □, C_i form.

Our conclusions are somewhat different from those proposed in previous publications. In those publications, a complete range of miscibility at high temperature and an only solid–solid domain for compositions rich in $C_{12}H_{22}O_4$ at low temperatures was pointed out. However, in another system of the same family studied by our group, the tetradecanedioic acid/hexadecanedioic acid binary system [16], certain similarities are observed, *i.e.*, at room temperature, also two $[C + C_i]$ domains are present, and upon heating, solid–solid and solid–liquid domains are related by peritectic and eutectic invariants, with the common point that all the phases are *C* (*P*21/*c*).

From a practical point of view, only alloys with a composition close to the components, or near the eutectic composition (*ca.* 50 mol-% of $C_{12}H_{22}O_4$) can be considered as suitable MAPCMs (molecular alloys as phase-change materials) for applications in the fields of energy storage and thermal protection. These can provide solutions at around 405, 399, and 382 K with a latent heat around 45 kJ/mol. This allows us to provide MAPCMs at temperatures where many of the molecular substances used as PCMs (unbranched alkanes and alkanoic acids) may not offer a solution.

This study was supported by the CICYT (MAT2005-07965-C02-01), *Grup Consolidat de Cristalografia* (2005SGR00764), and XeRMAE projects.

REFERENCES

[1] M. A. Cuevas-Diarte, N. B. Chanh, Y. Haget, *Mater. Res. Bull.* **1987**, *22*, 985.
[2] Y. Haget, *J. Chim. Phys.* **1993**, *90*, 313.
[3] D. Mondieig, A. Marbeuf, L. Robles, P. Espeau, B. Porier, Y. Haget, T. Calvet-Pallas, M. A. Cuevas-Diarte, *High Temp.–High Pressures* **1997**, *29*, 385.
[4] H. A. J. Oonk, D. Mondieig, Y. Haget, M. A. Cuevas-Diarte, *J. Chem. Phys.* **1998**, *108*, 715.
[5] Y. Haget, D. Mondieig, M. A. Cuevas-Diarte, Patent FR 91/08695, EP 92915596.8, and US 07/988,949.
[6] Y. Haget, D. Mondieig, M. A. Cuevas-Diarte, *Dépôt de marque ALCAL®*, Centre National de la Recherche Scientifique (France), 1993.
[7] D. M. Small, 'Handbook of Lipid Research', Plenum Press, New York, 1986.
[8] J. Housty, M. Hospital, *Acta Crystallogr., Sect. B* **1968**, *24*, 486.
[9] J. Housty, M. Hospital, *Acta Crystallogr.* **1966**, *21*, 553.
[10] N. B. Chanh, Y. Haget, J. Bèdouin, *J. Bull. Soc. Fr. Minéral. Cristallogr.* **1972**, *95*, 281.
[11] M. A. Cuevas-Diarte, Ph. D. Thesis, Universitat de Barcelona, 1978.
[12] A. D. Bond, M. R. Edwards, W. Jones, *Acta Crystallogr., Sect. E* **2001**, *57*, o141.
[13] V. R.Thalladi, M. Nüsse, R. Boese, *J. Am. Chem. Soc.* **2000**, *122*, 9227.
[14] M. Vanier, F. Brisse, *Acta Crystallogr., Sect. B* **1982**, *38*, 643.
[15] F. Kaneko, E. Ishikawa, M. Kobayashi, M. Suzuki, *Spectrochim. Acta, Part A* **2004**, *60*, 9.
[16] L. Ventolà, V. Metivaud, L. Bayés, R. Benages, M. A. Cuevas-Diarte, T. Calvet, *Helv. Chim. Acta* **2006**, *89*, 2027.
[17] E. von Sydow, *Acta Chem. Scand.* **1956**, *10*, 1.
[18] T. R. Lomer, *Acta Crystallogr.* **1963**, *16*, 984.
[19] T. Kobayashi, M. Kobayashi, H. Tadokoro, *Mol. Cryst. Liq. Cryst.* **1984**, *104,* 193.
[20] M. Goto, E. Asada, *Bull. Chem. Soc. Jpn.* **1978**, *51*, 70.
[21] R. Courchinoux, N. B. Chanh, Y. Haget, T. Calvet, E. Estop, M. A. Cuevas-Diarte, *J. Chim. Phys.* **1989**, *86*, 561.
[22] G. S. Pawley, *J. Appl. Crystallogr.* **1981**, *4,* 357.
[23] Materials Studio 3.2, developped by Accelrys in 2005.
[24] M. Hospital, Ph. D. Thesis, Université Bordeaux, 1964.
[25] Q. Gao, H.-P. Weber, B. M. Craven, R. K. McMullan, *Acta Crystallogr., Sect. B* **1994**, *50*, 695.

[26] A. Cingolani, G. Berchiesi, *J. Therm. Anal.* **1974**, *6*, 87.
[27] M. P. Doss, Technical and Research Division of the Texas Company, New York, 1952.
[28] M. Goto, E. Asada, *Bull. Chem. Soc. Jpn*. **1978**, *51*, 2456.
[29] F. Kaneko, M. Kobayashi, Y. Kitawgawa, Y. Matsuura, *Acta Crystallogr., Sect. C* **1990**, *46*, 1490.
[30] V. Vand, W. M. Morley, T. R. Lomer, *Acta Crystallogr.* **1951**, *4*, 324.
[31] S. Abrahamsson, E. von Sydow, *Acta Crystallogr.* **1954**, *7*, 591.
[32] R. F. Holland, J. R. Nielsen, *Acta Crystallogr.* **1963**, *16*, 984.
[33] R. G. Snyder, J. H. Schachtschneider, *Spectrochim. Acta* **1963**, *19*, 85.
[34] M. Kobayashi, T. Kobayashi, Y. Cho, F. Kaneko, *Makromol. Chem., Macromol. Symp.* **1986**, *5,* 1.
[35] R. F. Holland, J. R. Nielsen, *J. Mol. Spectrosc.* **1962**, *9*, 436.
[36] R. F. Holland, J. R. Nielsen, *J. Mol. Spectrosc.* **1963**, *16*, 902.
[37] N. Garti, E. Wellner, S. Sarig, *Kristall Technik* **1980**, *15*, 1303.
[38] K. Sato, M. Okada, *J. Cryst. Growth* **1977**, *42*, 259.

Received October 23, 2007